AJNR

Reformatted planar 'Christmas tree' MR appearance of the endolymphatic sac.

M C Oehler, D W Chakeres and P Schmalbrock

AJNR Am J Neuroradiol 1995, 16 (7) 1525-1528
http://www.ajnr.org/content/16/7/1525

Reformatted Planar 'Christmas Tree' MR Appearance of the Endolymphatic Sac

Mary C. Oehler, Donald W. Chakeres, and Petra Schmalbrock

Summary: A high-resolution three-dimensional Fourier transform technique and prototype bilateral dual phased-array surface coil technique was used to make inner ear structures visible on MR. Multiplanar reformatted images, parallel to the plane of the vestibular aqueduct, allowed viewing of the entire endolymphatic sac/vestibular aqueduct on one section, producing a "Christmas tree" shape. The reformation was obtained using a double oblique angle, 45° from true sagittal and 70° from the orbital-meatal axis.

Index terms: Magnetic resonance, three-dimensional; Temporal bone, magnetic resonance

Our goal has been to obtain high-resolution magnetic resonance (MR) images with signal-to-noise ratio and spatial resolution adequate to see the vestibular aqueduct/endolymphatic sac on one image and to allow better understanding of the endolymphatic system anatomy and function. Because the microscopic anatomy of the endolymphatic sac is complex, three-dimensional reconstructions of histologic sections have been helpful in defining the internal anatomy of the endolymphatic sac (1). Rather than representing one large confluent cavity, the endolymphatic sac is composed of multiple small channels that are interconnected (Fig 1). The appearance of the outer margins of this structure and these interconnected channels is like a sail or a Christmas tree.

Materials and Methods

We used a 3-D Fourier transform technique for high-resolution MR imaging (2, 3) of the inner ear structures using prototype bilateral dual phased-array coils (4) (Fig 2). Axial images were obtained on a 1.5-T imaging unit (General Electric, Signa, Milwaukee, Wis) using a 3-D GRASS (gradient recalled acquisition in a steady state) technique (24/6/1 [repetition time/echo time/excitations], 0.7 mm section thickness, 60 sections). The field of view was 18 cm with a matrix of 512 × 288 and a 40° flip angle (2, 3). The acquisition time was 7.5 minutes. Planar reformation images of the 3-D data set could be made in any plane using the standard reformation software on the imager and a tracker ball for graphic prescription. Images of the contents of the vestibular aqueduct were reformatted from the original axial images using multiple complex oblique angles.

We studied six volunteers, ranging in age from 17 to 47 years, three male and three female. In all subjects fluid signal intensity within the vestibular aqueduct was seen bilaterally; however, in two volunteers, the line of signal intensity was very thin so that detail was limited. On axial images, the signal within the contents of the aqueduct was seen only over short segments. It was usually better seen on the sagittal reformation as well as on the multioblique reformations.

The ideal imaging plane for parallel reformation of the contents of the vestibular aqueduct was found by first selecting a sagittal reformatted image through the vestibular aqueduct (Fig 2B) as a road map image. An oblique coronal reformation plane with an approximate 70° angle from the inferior orbital-meatal axis was chosen (5). This plane is in part parallel to the long axis of both vestibular aqueducts. Once the high signal intensity within the aqueduct was partially profiled over a long segment (Fig 2C), the reformation plane was rotated 45° toward the true sagittal plane, parallel to the posterior margin of the petrous portion of the temporal bone. The double oblique section intersects the region of the contralateral cavernous carotid artery. The plane was adjusted with the tracker ball to display as much of the vestibular aqueduct lumen as possible. The normal aqueduct lumen then was seen maximally (Fig 2D).

Received May 17, 1994; accepted after revision October 17.

Supported in part by National Institutes of Health grant R29DC01646-01A1.

Presented at the International Congress of Head and Neck Radiology, Washington, DC, 1994.

From the Department of Radiology, Ohio State University, Columbus.

Address reprint requests to Dr Mary C. Oehler, Assistant Professor, Department of Radiology, Division of Neuroradiology, Ohio State University, 410 W 10th Ave, Columbus, OH 43210.

AJNR 16:1525–1528, Aug 1995 0195-6108/95/1607–1525

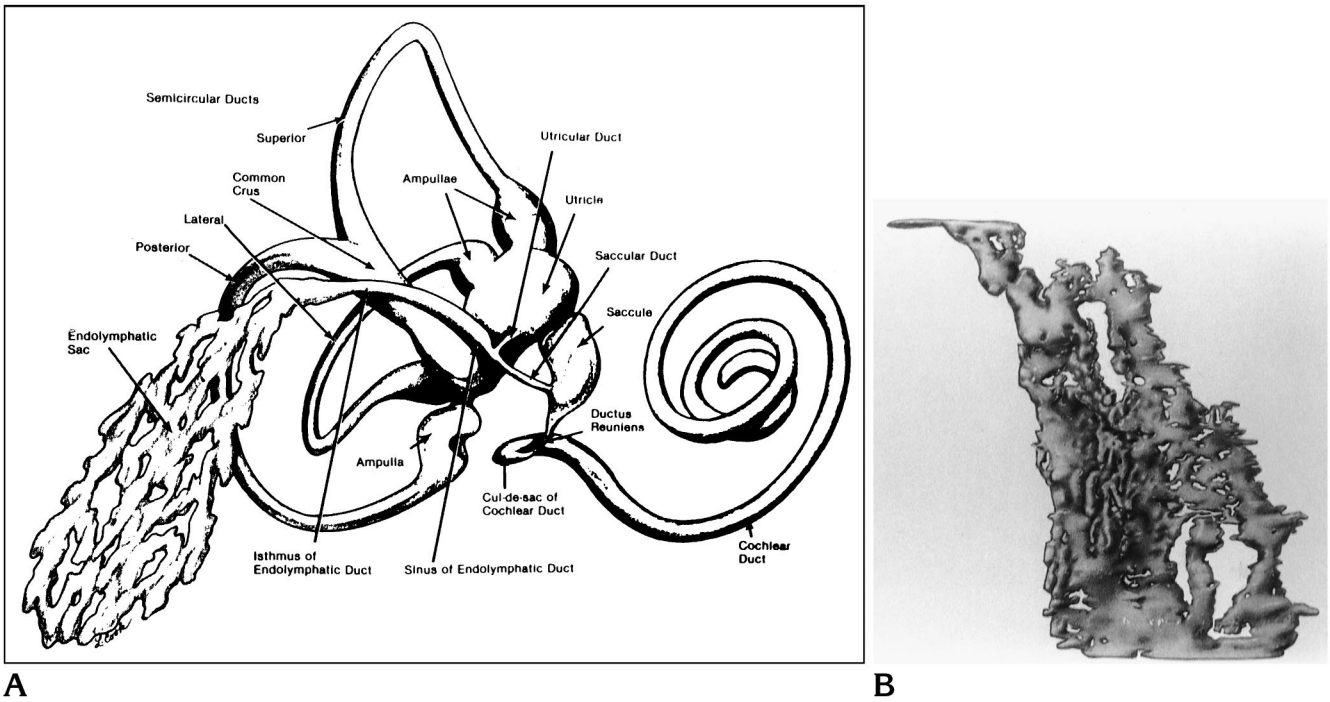

Fig 1. *A*, A diagram of the membranous labyrinth and its relationship to the endolymphatic duct and sac as viewed from a posterior perspective.

B, A diagram of computer reconstructions of histologic sections of a normal human endolymphatic sac. This image is not from MR imaging. Note that the endolymphatic sac is not a simple structure, but rather is composed of multiple sinusoidal cavities. The general conformation of the endolymphatic sac is like a sail or Christmas tree (from Schuknecht [1]).

Results

The normal endolymphatic sac has a "Christmas tree" appearance, with the top directed toward the endolymphatic duct and the base directed toward the jugular fossa. When the appropriate reformation is reached, the high-signal-intensity structures within the aqueduct point toward the common crus.

High signal intensity within the vestibular aqueduct was seen to some extent in all healthy subjects, but our images did not display the true sinusoidal nature of the endolymphatic sac as seen on actual histologic sections. The fluid and membranes in the vestibular aqueduct were seen as a fairly homogeneous structure of high signal intensity on these gradient-echo images, with signal similar to other fluid-containing structures such as the cochlea and vestibule. In general, the signal intensity was homogeneous with smooth margins, except in one subject who had bilateral notched defects in the medial aspect of the duct.

Fig 2. *A*, Axial high-resolution MR image of the left temporal bone, magnified four times. This is the primary image plane of acquisition. The plane parallel to the endolymphatic sac/vestibular aqueduct (ES) is approximately 45° from the true sagittal plane (*dotted white line*).

B, Reformatted sagittal image of the left temporal bone from the axial data set. The reformation plane from a coronal position is rotated approximately 70° to parallel the long axis of the ES (*dotted line*). This is used as the reference image for the first oblique coronal reformation.

C, The 70° coronal oblique MR image of the left temporal bone oriented from the sagittal reference in B.

D, This double oblique MR image is obtained by rotating the reformation plane parallel to the major axis of the left temporal bone. Starting from the position in C, the reformation plane is rotated approximately 45° parallel to the dotted line seen on A. After combining the sagittal and oblique angles, this is the "Christmas tree" appearance of the ES. Note that the ES has smooth straight margins and that the ES points towards the common crus. The stripes in the ES are most likely artifacts related to the reformation process.

Labeled structures include endolymphatic sac/vestibular aqueduct contents (*es*), posterior semicircular canal (*psc*), cochlea (*c*), facial nerve (*fn*), vestibule (*v*), superiorsemicircular canal (*ssc*), endolymphatic duct (*ed*), jugular fossa (*jf*), common crus (*cc*), and internal auditory canal (*iac*).

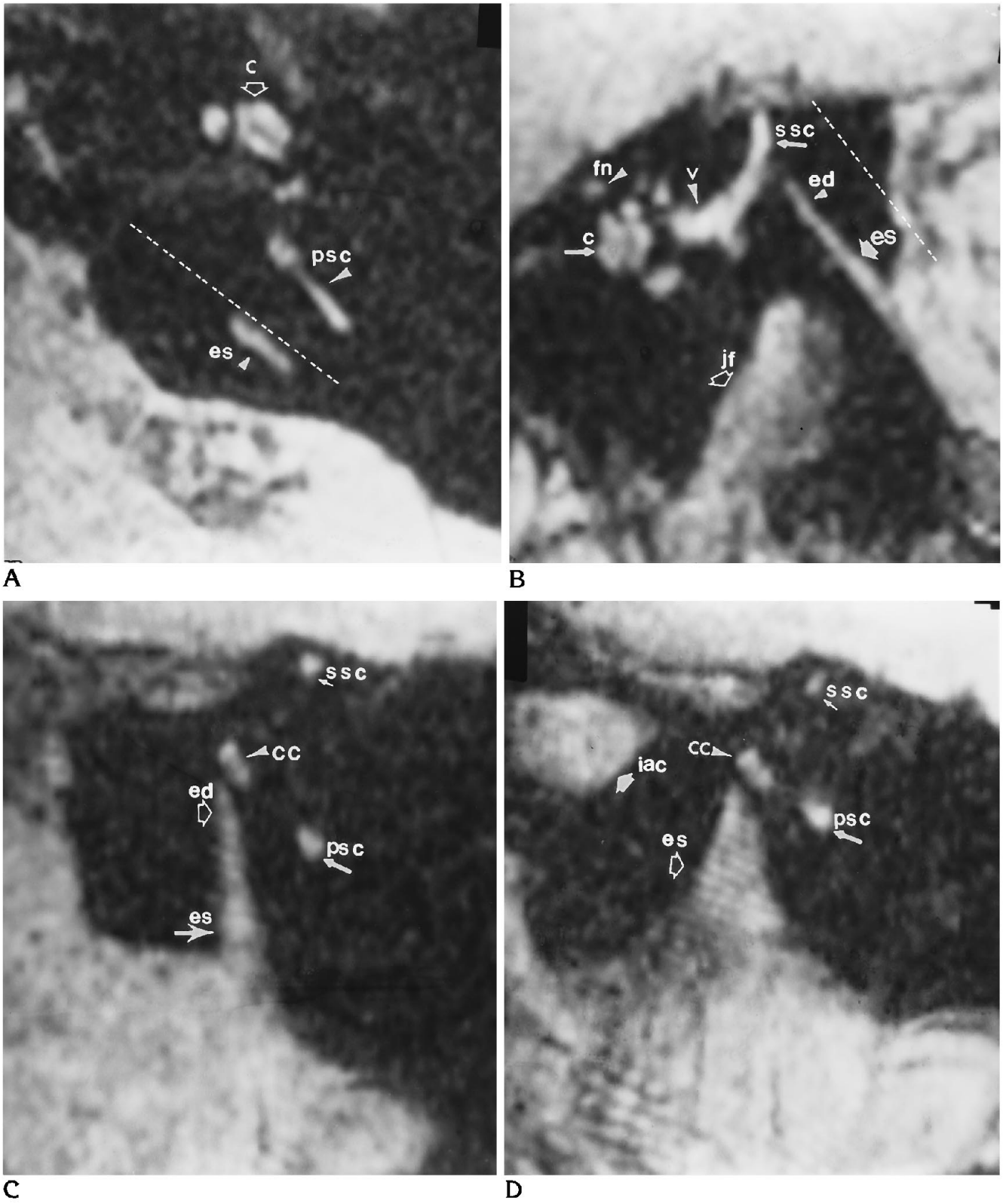
c
psc
es
A
ssc
fn
v
ed
c
es
jf
B
ssc
cc
ed
psc
es
C
ssc
cc
iac
psc
es
D

Discussion

The inner ear is composed of the membranous labyrinth surrounded by the outer bony labyrinth. The membranous labyrinth is composed of fine membranes and fluid spaces. The endolymphatic system is a closed system and is continuous through the cochlea, the vestibule, and the semicircular canals. All of these structures eventually communicate with the endolymphatic duct and endolymphatic sac.

Three-dimensional MR images of the inner ear have been shown to be helpful in depicting this complex anatomy (6). With 2-D multiplanar reformatting techniques, we are able to display much of the vestibular aqueduct and its contents in one image plane. Previously reported techniques have used an external processing computer and stereoscopic acquisitions (6). The advantage of our method is that reconstructions can be obtained from the routine high-resolution examination with standard software.

The anatomy of the vestibular aqueduct and its contents is difficult to evaluate, because the routine orthogonal image section planes display only small portions of the aqueduct. If the lumen of the aqueduct is visible on a single image, this may more accurately define its structure and allow for quantitative evaluation such as measurement of the area of the fluid-filled aqueduct, contour, and homogeneity. Subtle deformities of the contents of the vestibular aqueduct may be more obvious. Such quantitative studies may be important because the endolymphatic sac is thought to play a role in homeostasis of the inner ear (7). For example, Meniere disease may have more than one cause, but pathologically presents with cochlear and usually saccular hydrops. The endolymphatic space expands into the perilymphatic space with dilatation and herniation of Reissner's membrane occurring in many cases (8).

Computed tomography can show enlargement of the vestibular aqueducts, for instance, in the large vestibular aqueduct syndrome (9), but it is insensitive to subtle changes in the membranous labyrinth itself. In the large vestibular aqueduct syndrome, the primary pathophysiology may in fact be related to bone dysplasia with secondary enlargement of the endolymphatic structures. Although enlargement of the vestibular aqueduct and of the fluid contents of the aqueduct as seen on MR have been reported previously (10, 11), it remains to be seen whether obliteration of the endolymphatic sac can occur within a bone vestibular aqueduct of normal size. If the sac is obliterated long before there are comparable bone changes in the vestibular aqueduct, MR with visibility of the lumen of the aqueduct offers a theoretic advantage over high-resolution computed tomography. MR has shown loss of normal fluid within the posterior semicircular canal in a patient with Cogan syndrome and normal high-resolution computed tomography findings (11).

The imaging findings we have presented are very similar to the anatomic configuration of the endolymphatic sac as seen on computer reconstruction of histologic sections of the inner ear (Fig 1); however, the spatial resolution still is insufficient to distinguish the true sinusoidal nature of the duct or to confirm whether in fact all of the high signal intensity seen within the vestibular aqueduct represents the endolymphatic sac and its contents. Further improvement in spatial resolution would be required for a more detailed depiction of the vestibular aqueduct and for delineating the endolymphatic sac structures; however, with the current MR techniques, spatial resolution is limited by the available signal-to-noise ratio.

References

1. Schuknecht HF. *Pathology of the Ear*. Philadelphia: Lea & Febiger; 1993: 50–51, 45–47, 62, 64
2. Schmalbrock P, Brogan M, Chakeres D, et al. Optimization of submillimeter-resolution MR imaging methods for the inner ear. *J Magn Reson Imaging* 1993;3:451
3. Brogan M, Chakeres D, Schmalbrock P. High-resolution 3DFT MR imaging of the endolymphatic duct and soft tissues of the otic capsule. *AJNR Am J Neuroradiol* 1991;12:1–11
4. Schmalbrock P, Pruski J, Sun L, et al. Phased array RF coils for high-resolution MRI of the inner ear and the brain stem. *J Comput Assist Tomogr* 1995;19:8–14
5. Chakeres DW, Spiegel RK. A systematic technique for comprehensive evaluation of the temporal bone by computed tomography. *Radiology* 1983;146:97
6. Tanioka H, Shirakawa T, Machida T, Sasaki Y. Three-dimensional reconstructed MR imaging of the inner ear. *Radiology* 1991;178: 141
7. Kuhn TK, Ikeda K, Morizino T, Murphy M. Pathophysiology of inner ear fluid imbalance. *Acta Otolaryngol* 1991;(suppl)485: 9–14
8. Paparella MM. Pathogenesis and pathophysiology of Meniere's disease. *Acta Otolaryngol* 1991;(suppl)485:26–35
9. Mafee MF, Charletta D, Kumar A, Belmont H. Large vestibular aqueduct and congenital sensorineural hearing loss. *AJNR Am J Neuroradiol* 1992;13:805–819
10. Hirsch BE, Weissman JL, Curtin HD, Kamerer DB. Magnetic resonance imaging of the large vestibular aqueduct. *Arch Otolaryngol Head Neck Surg* 1992;118:1124–1127
11. Casselman JW, Kuhweide R, Ampe W, Meeus L, Steyaert L. Pathology of the membranous labyrinth: comparison of T1- and T2-weighted and gadolinium-enhanced spin-echo and 3DFT-CISS imaging. *AJNR Am J Neuroradiol* 1993;14:66–68